Egypt. J. Chem. **Vol. 68**, No. 11 pp. 543 - 555 (2025)

Egyptian Journal of Chemistry

http://ejchem.journals.ekb.eg/

An Easy and Simple Approach for Biosynthesis of Selenium Nanoparticles; Characterization, Radiolabeling and Biomedical Application

Heba I. Elkouly[a*], Zainab S. Nasr[b] and Mohamed K. Hassane[b*]

[a] *Botany & Microbiology Department, Faculty of Science, Al-Azhar University (Girls Branch), Cairo, Egypt, P.O.11754.*

[b] *Labeled Compounds Department., Hot Labs Center, Egyptian Atomic Energy Authority (EAEA), Cairo, Egypt.*

Abstract

Nanomaterials biogenic approaches of synthesis exceed chemical ways in simplicity, toxicity and generation of homogeneous colloidals. Herein, a rare approach for biosynthesis of SeNPs is described where a rapid myogenic method was applied. The endophytic fungus isolate, *Asperigillus terrus* H1 with accession no. PQ550684, that isolated for the first time from *Rumex thyrsiflorus* was used for the bio-reduction of sodium selenite contained in the growth medium to produce selenium nanoparticles. Change in color of the culture medium to orange-red signifies the formation of nano-selenium. DLS, TEM and ICP-OES techniques demonstrated the formation of monodispersive amorphous selenium nanoparticles with average hydrodynamic size of 55.76 nm with -25.6 particles charge. The synthesized SeNPs were checked for them *in-vitro* cytotoxicity against normal human lung fibroblast cells (MRC-5) and human lung adenocarcinoma cell line (A549) which giving IC_{50} of 485.16±13.71 and 196.25± 4.23 µg/ml respectively. Their ability to be applied in biomedical applications was studied *in-vivo* through labeling them with ^{99m}Tc and tracing their distribution in normal and tumor-bearing mice. The produced mycogenic SeNPs showed excellent physical and biological characteristics that could make them a promising nanoplatform for tumor molecular imaging.

Keywords**:** Biogenic nanoparticles; Selenium; endophyte *Asperigillus terrus* H1; Tumor Imaging; Radiolabeling

1. Introduction

Nanotechnology is regarded as one of the most important new topics in material science in terms of nanomaterial applications and production [1]. Materials at the nanoscale range in size from 1 to 100 nm and have distinct chemical, physical, and properties [2]. The semi-metallic element selenium (Se) belongs to the chalcogen family. Perior to the discovery that many living things, including mammals, depend on it for essential functions, it was believed to be hazardous [3,5]. Naturally, it might be found in different oxidation states, which include elemental state $(Se)^0$, inorganic forms like selenite (Na_2SeO_3) and selenite (Na_2SeO_4), and organic forms like selenomethionine (SeMet) and selenocysteine (SeCyt) [6, 7].

Researchers are starting to grasp how crucial selenium is for bio- research, given that it is a required component of various antioxidant enzymes, as glutathione peroxidase (GPx) [7]. It is critical in protecting physiological tissues from cellular oxidative stress, which causes aging-related diseases and cancers [8, 9]. The fact that selenium is inert, less poisonous, and less immunogenic than other common elements such as gold and silver helps to explain its biocompatibility in vivo. Furthermore, as Se degrades in vivo, degraded Se might function as anti-proliferative agents against numerous types of tumor cells while still also, providing nutrients to other regular cells [9,11].

Fungi can produce large amounts of proteins that help increase the productivity of SeNPs [10]. Although extracellular mycosynthesis of SeNPs has been reported using many molds such as *Aspergillus niger* and *Penicillium sp.* [11], there aren't enough reports on the mycosynthesis of SeNPs by endophytic fungi, which colonize the internal tissues of plants in a mutualistic relationship and are considered a potential source of bioactive compounds [12].

Selenium has powerful antimicrobial properties on its own because numerous studies have documented how efficiently it inhibits the growth of several bacteria and fungi for example sodium selenite (Na2SeO4), was feasible to completely block the development of *Alternaria brassicicola* and *Fusarium sp.* [12,13]. Antifungal, antimicrobial, and anti-parasitic properties have also been reported for SeNPs [14]. Moreover, SeNPs have antioxidant activity, immunological balance and cancer prevention capacities [15,18].

In addition to consuming less energy and creating uniform nano-sized particles, the biological production of nanomaterials offers various advantages over chemical or physical methods [19]. In addition to their redox capabilities, they could develop such nanomaterials with decreased metal toxicity since certain mycogenic nanoparticles can operate as nanozymes that simulate enzymes like peroxidase [20]. In comparison to bacteria, there are numerous benefits to using fungi in nanoparticle synthesis the

*Corresponding author e-mail: heba.ibrahim@azhar.edu.eg.; (Heba I. Elkouly).

Receive Date: 27 November 2024, Revise Date: 13 February 2025, Accept Date: 25 March 2025

DOI: 10.21608/ejchem.2025.338679.10892

procedure is simple to scale up and economically feasible; the resulting nanoparticles are highly efficient, monodispersed, and have good morphologies; additionally, fungi-mediated synthesis is ecologically friendly [21].
Selenium nanoparticles outperform other forms of the element in terms of biocompatibility, antioxidant activity, and in vivo absorption, such as selenite (SeO_3^{-2}), Selenate (SeO_4^{-2}), and organo-selenium compounds [22], they may also be readily functionalized by conjugation with molecules [23].
Every plant has microorganisms living inside its tissues that produce metabolites; these are known as endophytes if their presence does not result of harmful effect to the plant [24, 25]
Endophytes have been isolated from plants in every taxon that has been studied thus far, and they can be found in every habitat on the planet. The explanation of endophyte/host plant cross-talk has garnered more attention in recent years due to the potential benefits of these connections for humans [26].
This study's primary goal was to isolate endophytic fungi from wild plants that have ability for the myco-synthesis of selenium nanoparticles. After complete characterization of the synthesized SeNPs, their readiness for biomedical applications was assessed by radiolabelling them with technetium 99m (^{99m}Tc) and observing their pharmacokinetics in normal and tumor-bearing mice. The results obtained demonstrated promising findings and revealed that the mycogenic SeNPs could be used as a solid tumor imagin

2. Experimental

2.1. Materials and Equipment:

Sodium selenite (Na_2SeO_3, MW: 172.94 g/mol) with purity ≥ 98%, sodium dithionite ($Na_2S_2O_4$, MW: 174.107 g/mol), potato dextrose (PD), and glucose yeast peptone (GYP) media were purchased from Sigma Aldrich Company, St. Louis, Mo., USA. Dialysis membrane cutoff of 3500, Whatman No. 1 paper chromatography was purchased from Whatman International Ltd. (Maidstone, Kent, UK). A 0.22 µm filter membrane from Millipore, USA). Technetium-99m was obtained as sodium pertechnetate in saline elute ($Na^{99m}TcO_4$) from a $^{99}Mo/^{99m}Tc$ generator acquired from the Egyptian Atomic Energy Authority (EAEA). All chemicals and organic solvents used were of analytical and HPLC grade, respectively; in addition, all aqueous solutions were prepared in bidistilled water. HR-TEM (Ted Pella, CA, USA) to detect the shape and size of particles. Zetasizer (Malvern Instruments Ltd., Malvern, UK) for the determination of hydrodynamic diameter distribution, zeta potential, and polydispersity index. Inductively coupled plasma (ICP-OES, Perkin Elmer Optima 5300 DV, Massachusetts, U.S.) NaI (Tl) γ-ray scintillation counter (SPECTECH, ST450 SCA, USA) was used for measuring radioactivity.

2.2. Methods

2.2.1. Sampling and endophyte fungal isolation

A healthy fresh plant samples were collected from Elbehira governorate, Egypt. The samples were numbered, transported in an icebox to Ecology Laboratory, and identified by Prof. Dr. Albara Salaheldin, at Al-Azhar University, Faculty of Science (boys branch), Cairo, Egypt.
The plant parts surfaces were sterilized as previously mentiond by Elkhouly etal. (2021) [27]**.** Briefly, the plant parts were sterilized by rinsing with sterile distilled water (SDW), followed by dipping in to 70% ethanol for 1 min, the pieces were again rinsed in SDW then immersed in 2% sodium hypochlorite for 1 min followed by rinsing with SDW triply. The sterilized parts were allowed to dry in laminar flow, and a healthy leafs were cut into small pieces of 1 to 2 cm^2 and placed on potato dextrose agar medium (PDA) plate for approximately 5 days to investigate the growth of any endophytic fungi [27, 28]**.** The grown fungal colonies were purified and screened for selenite tolerance and reduction by growth on solid PDA medium containing 2 µg sodium selenite (Na2Se2O3) for 7 days. The higher fungal growth with red coloration suggested the higher selenite reducing strains that were selected for subsequent experimentations.

2.2.2. Biosynthesis of SeNPs by *isolated endophytic fungi*:

The most potent endophyte isolate was used for mycosynthesis of the Se NPs. About 100 ml of sterile GYP medium containing 5.2 gm of sodium selenite was prepared and transferred to a sterile 250 ml Erlenmeyer flask.The medium was inoculated with 1 ml of the fresh inoculum (OD 600) and incubated aerobically at 28 °C in a shaker incubator at 150 rpm. After 7 days in the dark, the medium turned orange red color, and then the fungal growth pellets were removed from the culture medium by centrifugation at 4000 rpm for 10 min. The supernatant was filtered through a 0.22 µm filter membrane. For the separation of SeNPs, the culture supernatant was dialyzed three times against distilled water for 12 hours and stored colloidal in aqueous medium at the refrigerator for further characterization. Two positive controls of the fungal culture filtrate (FCF) and un inoculated culture media and a negative control of only sodium selenate solution were maintained under the same conditions [29, 30].

2.2.3. Genetic identification of endophytic fungus

Here, 18S rRNA analysis was performed on the endophyte fungus by biosynthesing Nano selenium particles, DNA was extracted using Qiagen DNeasy Mini Kit protocol, amplified using two universal primers ITS1 (5′-TCCGTAGGTGAACCTGCG-3′) and ITS4 (5′- TCCTCCGCTTATTG ATATGC-3′) and sequenced by Macrogen Companies, Seoul, South Korea. To identify the homology and similarity of the obtained sequence, it was aligned with known sequences available at gene bank using BLAST tool available online (https://blast.ncbi.nlm.nih.gov/Blast.cgi). The phylogenetic tree was constructed using by MEGA 11 program according to Kumar *et al*. (2016) [31]**.** The resulting gene sequence was submitted to the NCBI GenBank database and an accession number was attained.

2.2.4. Characterization of produced SeNPs:
The prepared SeNPs were then characterized for their physical properties. Zetasizer DLS was recruited to determine their hydrodynamic diameter and zeta potential, while their shape and core sizes were determined by HR-TEM. In order to confirm that the formed nanoparticles are SeNPs, ICP-OES is used since SeNPs have no spectrum in UV-Vis regions [32, 33].

2.2.5. In vitro biological evaluation of SeNPs (cytotoxicity and anticancer activity):
Upon characterization, the produced SeNPs were evaluated *in vitro* using viability assays (MTT assay). The cytotoxicity of SeNPs was tested against normal human lung fibroblast cells (MRC-5) and human lung adenocarcinoma cell line (A549) at the Regional Centre for Microbiology and Biotechnology, Cairo, Egypt, according to Mosmann (1983) [34] . All cell lines used were provided from the American type culture selection (ATCC, Rockville, MD). The cells were grown in RPMI-1640 medium supplemented with 50 g/mL gentamycin and 10% activator fetal calf serum that was purchased from Lonza (Belgium). The cells were subcultured every two days and incubated in 5% CO2 at 37 °C.

2.2.6. Radiolabelling of SeNPs with ^{99m}Tc:
For performing a distribution study of the produced SeNPs *in vivo*, SeNPs were radiolabeled to prepare the tracer. SeNPs were radiolabeled with ^{99m}Tc directly in presence of dithionite as a reducing agent. Practically, 25 mg of $Na_2S_2O_4$ was added to a dry and clean penicillin vial, and then 100 µl of a fresh elute of $Na^{99m}TcO_4$ (200 MBq) was added. The vial was shaken well till all dithionite dissolved, then 1 ml of the colloidal containing SeNPs was added to the mixture. The percent radiochemical yield (RCY%) of ^{99m}Tc- SeNPs was determined using ascending paper chromatographic technique with acetone as the mobile phase and NaI (Tl) γ-ray scintillation counter [35,36]. The procedure was optimized using varying SeNPs and dithionite concentrations and pH values to get a maximum yield of ^{99m}Tc- SeNPs. [37, 38].

2.2.7. Purification of ^{99m}Tc-SeNPs:
Radiochemical purification of ^{99m}Tc-SeNPs was achieved by loading the final mixture onto a PD10 column (Sephadex G-25 gel filtration) and using 0.05M phosphate buffer (pH 7.4) as the eluent. Fractions of 1.5 ml were collected and counted by a NaI (Tl) γ-ray scintillation counter [39, 40].

2.2.8. *In-vitro* stability study of ^{99m}Tc-SeNPs:
To investigate the radiolabeling tolerance in physiological conditions, the stability of ^{99m}Tc-SeNPs was estimated *in-vitro*. Difinitely 100 µl from the purified ^{99m}Tc-SeNPs portion was incubated with 0.9 ml of normal mice serum for 24 h at 37°C. RCY% was determined by the same paper chromatographic method described above at different time intervals [41].

2.2.9. Evaluation of *In-vivo* studies of ^{99m}Tc-SeNPs
All animal experiments total of 30 mice were conducted in accordance with the ethical rules and principles for animal care that are proposed by the Research Ethics Committee (REC/NCRRT), EAEA, Egypt. Normal and solid tumor-bearing Swiss albino mice of weight 25–35 g were provided from the National Cancer Institute, Egypt. They were allowed to freely access food and water at room temperature, 12 hour light/dark environment [42]. For distribution study on normal mice, they were injected by ^{99m}Tc-SeNPs intravenously (I.V.) with a dose of about 5 MBq/100 µl *via* the tail vein. Tumor bearing mice were also injected intravenously with the same dose as normal ones. Mice were weighted and sacrificed by ether anesthesia at 15, 30, 60, 90 and 120 minutes post-injection time intervals [43]. Three mice were tested at each time point, their organs, blood, bone, muscles, and tumor tissues–in the case of tumor bearing mice–were removed, weighted, and counted using a NaI (Tl) γ-ray scintillation counter [38, 44]. Counted values were processed to calculate the organ's percentage injected dose per gram of tissue weight (% ID/g), using the following formula [37].

$$\%\ \mathrm{ID/g} = \frac{counts\ per\ gram\ organ}{counts\ dose\ given}\ x\ 10$$

Statistics
The recorded data were reported as the mean of triplicate measurements plus or minus the standard deviation. Significant differences were found using the analysis of variance (One-way ANOVA) test, followed by Duncan's test at *P*.

3. Results

3.1. Sampling and endophyte fungal isolation
In the current study, two endophyte fungi have been isolated from leaf parts of the plant sample as recorded in table (1). the plant sample have been identified by Prof. Dr. Albara Salaheldin as *Rumex thyrsiflorus* that growing in Egypt (El Beheira Governorate), Rumex genus (sorrel), belonging to the Polygonaceae family, Several species are used traditionally either as foods (soup or salad) or as healing agents [45]**.** The aerial parts, leaves and roots of the plant are used in traditional medicine. It is the first study to isolate endophyte from *Rumex thyrsiflorus* plant.

Table 1: Endophytic isolates from *Rumex thyrsiflorus*

Host plant	Plant part	Endophyte	Location of Plant
Rumex thyrsiflorus	Leaf	MPF1	31°03'46.0"N 30°35'02.0"E
		MPF2	

3.2. Biosynthesis of Selenium Nanoparticles (SeNPs) by the most potent strain:

A common technique for testing microbiological isolates for the production of selenium nanoparticles is color change observation [46]. The screening revealed that the most potent Myco-SeNPs producer was MPF2, in which the color of samples converted from colorless to redish orange. This indicate that, isolate MPF2 has great ability for convertion of sodium selenite to **Selenium Nanoparticles,** a combination of 100 ml of fungal growth at a temperature of 28 °C for a 7-day incubation period and 150 rpm shaking speed in the dark were the optimum conditions (Fig. 1)**.** To gather the developed SeNPs, a filtration step was done by Whatman Paper No. 1. The SeNPs filtrate was dialized using a 3500-cut-off dialysis bag against double distilled H_2O at room temperature for two days, then the characterization was performed. The obtained SeNPs were still suspended and did not aggregate for more than one month, indicating that a stable colloidal was prepared.

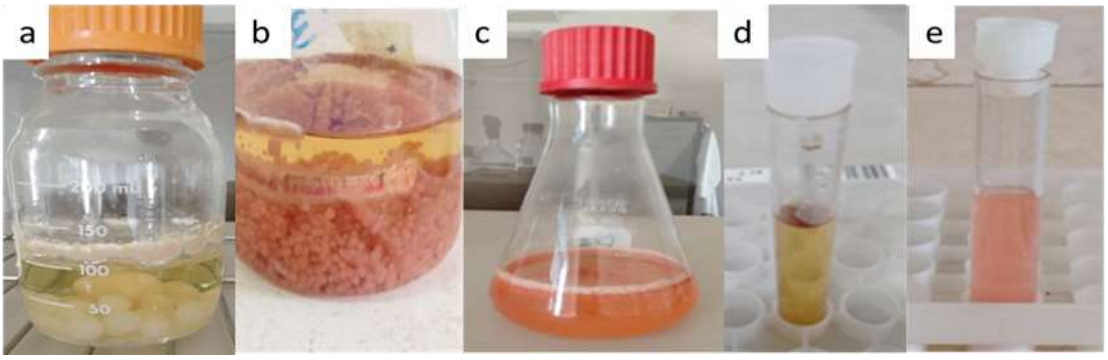

Fig. 1. Mycosynthesis of SeNPs by endophytic isolate MPF2 (a) *MPF2 isolate* pellet homogenized in enrichment GYP medium with Na_2SeO_3, (b) pellets of *MPF2* after incubation in darkness for 7 days at temperature of 28 °C and 150 rpm condition, (c) filtrate of *MPF2* supplemented with SeNPs, (d) the combination of GYP medium and Na_2SeO_3 showing a yellow color, (e) the orange red color of SeNPs after dialysis.

3.4. Genotypic identification of endophyte fungal isolate

The sequence of 18S rRNA gene for the isolate MPF2 was obtained, identified and aligned against other identified sequences available in the GeneBank database using BLAST tool to identify the similarity score and to calculate the statistical significance of the matches (http://www.blast.ncbi.nlm.nih.gov/Blast). The obtained result indicates close similarity of the 18S rRNA gene sequence with 73 % homology of the endophyte isolate with *Aspergillus terreus*. The phylogenetic analysis and tree were constructed using the neighbour-joining method (Fig. 2) by MEGA 11 program according to Kumar *et al*. (2016) [31]. According to the analysis of DNA sequence of endophye isolate MPF2 was identified as *Aspergillus terreus* H1 and deposited in GeneBank database with the accession no. PQ550684.

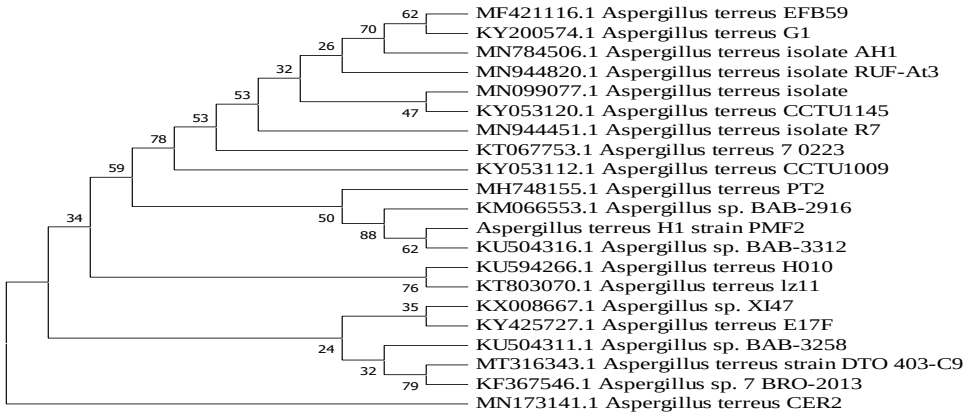

Fig. 2. Constructed phylogenetic tree of *Aspergillus terreus* H1

3.5. Particulate characterization of produced SeNPs particles:

About 90% of the particle diameters were within the range of 25–60 nm; with an average diameter of 55.26±4 nm according to the DLS diagram that demonstrated a relatively narrow hydrodynamic size distribution (Fig 3a). The zeta potential of SeNPs was negative charged of (−25.6 mV at pH 7) indicating a relatively stable colloidal was obtained. The stability of the produced SeNPs was confirmed virtually as they still colloidal in the aqueous medium without any sedimentation for more than one month under refrigeration. The stabilization of SeNPs may be attributed to the electrostatic repulsion between SeNPs generated by the highly negative surface charge of *A.terreus* H1 metabolites capping SeNPs [47].

HR-TEM images showed amorphous particles varying in their core sizes with a mean of 22.53±3 nm (Fig 3b)**.** However, ICP-OES showed two intense peaks at selenium wavelength window of 196 nm with a concentration of 5.5 mg/ml. (Fig 3c).

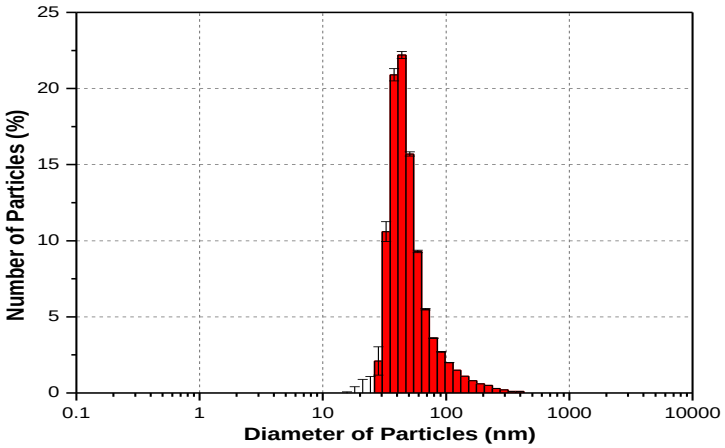

Fig. 3a DLS pattern of SeNPs produced *A.terreus* H1.

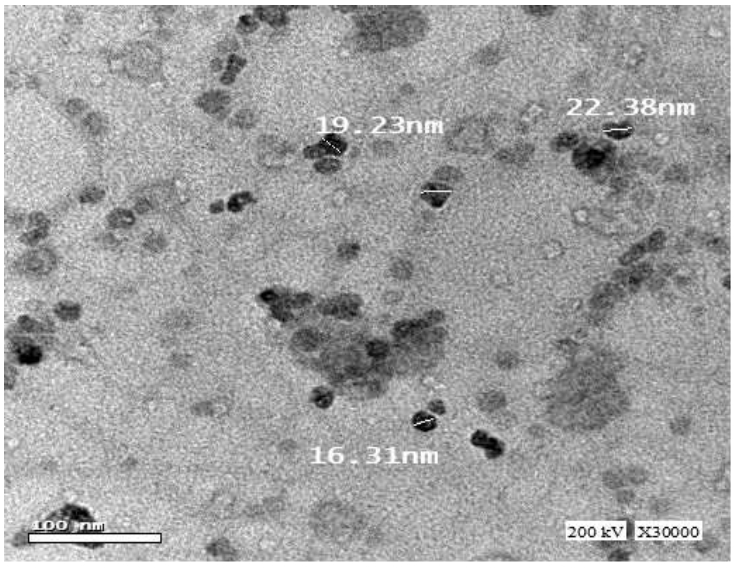

Fig. 3b HR-TEM of SeNPs produced *A.terreus* H1**.**

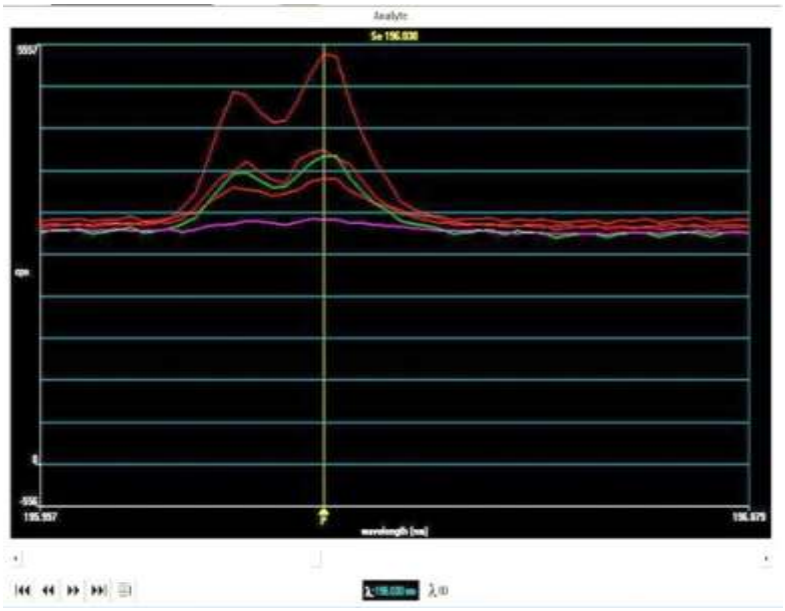

Fig. 3c ICP-OES analysis of SeNPs generated by *A.terreus* H1

3.6. In vitro evaluation of cytotoxicity and anticancer activity of SeNPs:

The results reveal that the SeNPs showed significant anti-proliferation activity against *lung carcinoma cells* (A549) with an IC_{50} value of 196.25± 4.23 µg/ml, and a maximum inhibitory suppression was observed up to 85.44% for SeNPs at a concentration of 500 µg/ml, as shown in (**Fig. 4a)**. While the IC_{50} value of 485.16±13.71 µg/ml for SeNPs against *normal human lung fibroblast cells* and a maximum inhibitory suppression were observed up to 52.09% for SeNPs at a concentration of 500 µg/ml, as shown in (**Fig. 4b**).

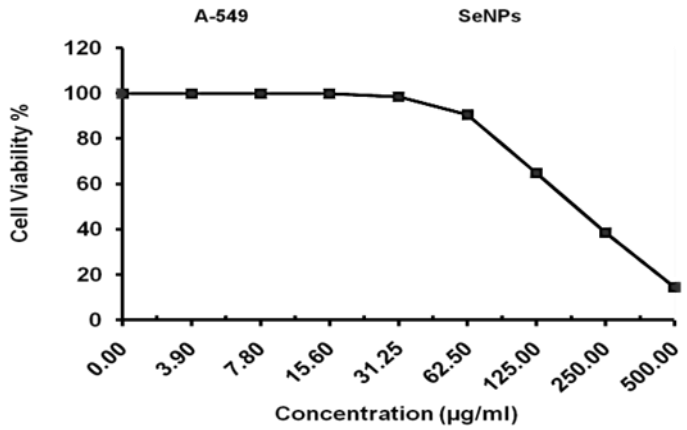

Fig. 4a IC_{50} of SeNPs anticancer activity against *Lung carcinoma cells.*

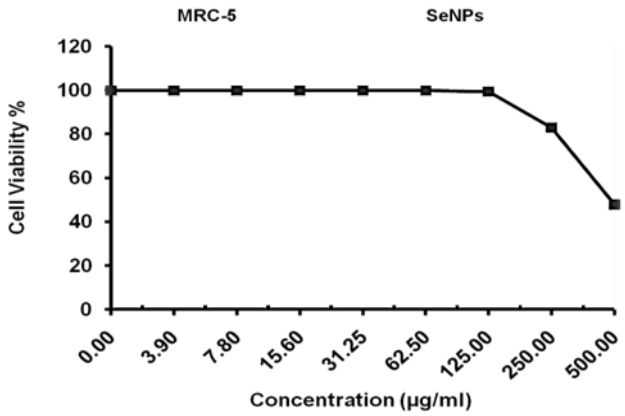

Fig. 4b IC_{50} of SeNPs cytotoxicity against *Normal lung fibroblast cell*.

3.7. Radiochemical yield and purification of ^{99m}Tc-SeNPs:

After optimizing SeNPs and dithionite concentrations and pH values, the maximum percent radiochemical yield (RCY%) of ^{99m}Tc-SeNPs determined by ascending paper chromatography has reached to 98.5 ± 0.5 using 2ml SeNPs and 25 mg sodium dithionite in pH 7 for 1 min reaction time at room temperature (Figs. 5 a,b,c). Using acetone as the developing solution, only free pertechnetate ($^{99m}TcO_4^-$) would migrate to the front of the strip while ^{99m}Tc-SeNPs would be remained at the spotting line.

By using gel filtration chromatography technique, particles with larger sizes are eluted firstly [48]. (Fig. 5d) shows the radiochemical purification of ^{99m}Tc-SeNPs using Sephadex G-25 column as a stationary phase and phosphate buffer of pH 7.4 as the eluent. At fractions 3-5, a radioactive and orange fraction corresponded to ^{99m}Tc-SeNPs was eluted free $^{99m}TcO_4^-$ appeared at fractions 9-10.

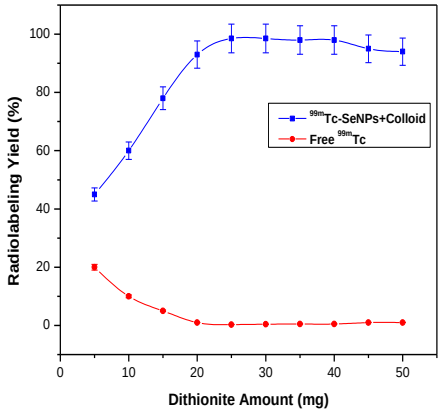

Fig. 5a Radiolabeling yield of ^{99m}Tc-SeNPs as a function of sodium dithionite amount.

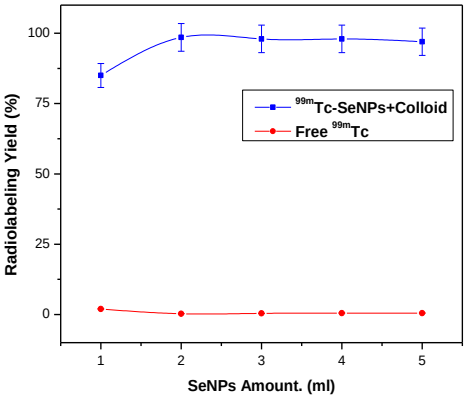

Fig. 5b Radiolabeling yield of ^{99m}Tc-SeNPs as a function of SeNPs amount.

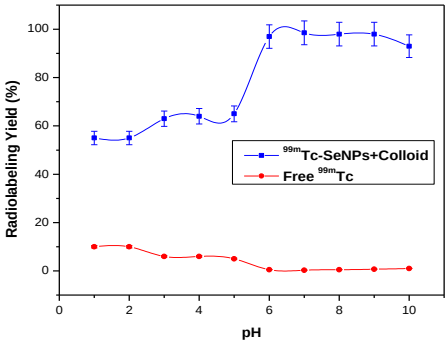

Fig. 5c Radiolabeling yield of ^{99m}Tc- SeNPs as a function of pH.

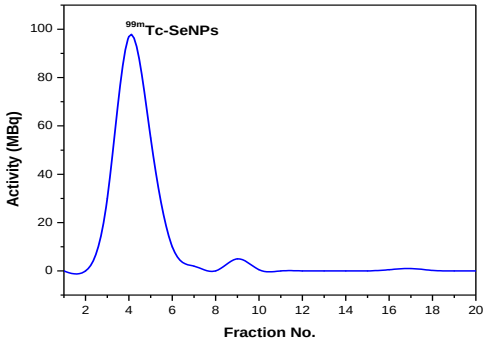

Fig. 5d Radiochemical purification of ^{99m}Tc-SeNPs using sephadex G-25 column

3.8. In-vitro stability of ^{99m}Tc-SeNPs:

The *in-vitro* stability of ^{99m}Tc-SeNPs was assessed in normal mice serum [49, 50]. (Fig. 6) shows that sufficient radiolabeling yield of ^{99m}Tc-SeNPs of 98% was up to 6 h, while after 12 h of incubation, less than 20% of ^{99m}Tc-SeNPs had released $^{99m}TcO_4$.

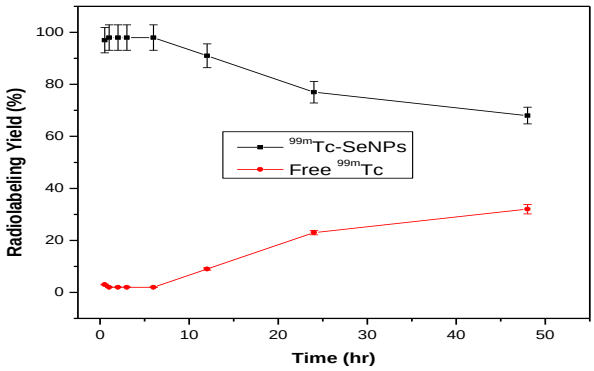

Fig. 6 *In-vitro* stability of ^{99m}Tc-SeNPs was assessed in normal mice serum at 37 ^{O}C.

3.9. Evaluation of *In-vivo* studies of ^{99m}Tc-SeNPs

3.9.1. Biodistribution in normal mice:

Distribution of nanoparticles mainly depends on the particles size and the capping agent [51]. Data presented in (Table 2) showed liver with maximum %ID/g of 22.37±4% in at 60 min post-injection (p.i.) with no significant accumulation in spleen, which means that due to the low particles sizes of the produced SeNPs, they could escape from reticuloendothelial organs allowing them to spend more time with circulation. In kidneys, about 11.84±2 %ID/g of at 60 min p.i., which confirmed that clearance of ^{99m}Tc-SeNPs was *via* urinary tract [17, 18, 52, 53].

Table 2 Biodistribution of ^{99m}Tc-SeNPs in normal mice at different time intervals *via* Intravenous injection; I.V. (Data represented as % ID/g ± SEM, n=3).

	% Dose/gram organ at time intervals post injection (min)				
Body Organs	**15**	**30**	**60**	**90**	**120**
Blood	38.75±7.7	3.3±0.7	4.26±0.9	5.79±1.2	4.28±0.9
Heart	0.91±0.2	3.84±0.8	2.68±0.5	2.97±0.6	2.47±0.5
Lungs	8.05±1.6	4.58±0.9	2.34±0.5	3.07±0.6	2.67±0.5
Liver	2.97±0.6	5.55±1.1	22.37±4.1	8.2±1.6	2.54±0.5
Spleen	0.0±0.0	1.75±0.4	1.09±0.2	1.37±0.3	1.39±0.3
Stomach	0.0±0.0	3.34±0.7	3.0±0.6	6.08±1.2	6.76±1.4
Intestine	0.0±0.0	1.39±0.3	1.3±0.3	1.94±0.4	2.76±0.6
Kidneys	10.71±2.1	11.56±2.3	11.84±2.5	9.32±1.9	9.33±1.9
Muscles	0.3±0.1	0.39±0.1	0.31±0.1	0.68±0.1	1.89±0.4
Bone	0.3±0.1	0.38±0.1	0.2±0.0	0.14±0.0	0.46±0.1

3.9.2. Biodistribution in solid tumor-bearing mice:

^{99m}Tc-SeNPs was injected I.V. route in tumor bearing mice in order to determine the target non-target ratio (T/NT, % ID/g of tumor divided by % ID/g of muscles). (Table 3) shows the maximum T/NT value with 5.65 after 30 min p.i. Higher accumulation of ^{99m}Tc-SeNPs in tumor tissues than normal muscles could be attributed to passive targeting due to the enhanced permeability and retention properties through leaky tumor tissues [53].

Table 3 Percentages of ID/g, for T/NT of ^{99m}Tc-SeNPs in solid tumor bearing mice at different time intervals *via*; I.V. injection (% ID/g ± SEM, n=3).

Body Organs	% Dose/gram organ at time intervals post injection (min)				
	15	**30**	**60**	**90**	**120**
Muscles (NT)	0.52±0.1	0.32±0.1	0.34±0.0	0.29±0.1	0.18±0.0
Tumor (T)	1.43±0.2	1.81±0.4	1.66±0.3	0.73±0.1	0.51±0.1
T/NT	2.75	5.65	2.83	2.81	2.52

4. Discussion:

Mycogenic nanomaterials can develop extracellularly, intracellularly, on dead biomass, or in biomass-free reactive culture filtrates. They are also connected with cell walls and surface materials. Metal can be sorbed onto cell walls and exopolysaccharide (EPS), creating nucleation sites for future mineral production. The type of nanomaterials generated can be determined by redox processes and the availability of ligands, metabolites, and organic molecules. Secreted amino acids, proteins, and autolysis products can all have an impact on the development and size of newly produced nanomaterials. Some ligands, such as phosphate, carbonate, and sulfide, may be the outcome of fungal metabolism and mineral dissolution. Metal transfer across the plasma membrane can cause intracellular vacuolar compartmentation, sequestration by intracellular acromolecules such as metallothionein and phytochelatins, and redox reactions of accumulated metal. Intracellular migration of nanoparticles to the cell membrane or cell wall, or exocytotic ejection to the outside, is indicated by [54, 55].

Fungal-mediated synthesis of nanoparticles has various benefits, but there are still unanswered challenges throughout the creation process, such as the involvement of fungal metabolites in size and shape regulation, the efficiency of biorecovery or pollutant degradation in real applications, as well as the potential for toxicity within the production system. Employing fungi in nanoparticle manufacturing has various advantages over employing bacteria. The technique is straightforward to scale up and economically

practical; the resultant nanoparticles are highly efficient, monodispersed, and have excellent morphologies; and fungi-mediated synthesis is environmentally friendly [21].

The use of endophytic fungi in this respect has emerged as rare and new approach for green and cost-effective production of several nanoparticles, in this study two fungal endophytes isolated from wild plant *Rumex thyrsiflorus* one of them *Aspergillus terreus* H1 has excellent ability for biotransformation of sodium selenite ($Na_2Se_2O_3$) to selenium nanoparticles within 7 days, This results similar to Gharieb et al. (2023) isolated two endophytic fungi from two wild plants *Catharanthus roseus* (periwinkle) and *Euphorbia milli* (crown of thorns), that identified as *Penicillium citrinum* and *Rhizopus arrhizus* .these fungal strains exhibited tolerance up to 40 Mm $NaSeO_3$ accompanied with red coloration of the medium that suggested selenite reduction and formation of selenium nanoparticles SeNPs [30]**.**

Various studies indicated that, the biosynthesis of SeNPs via both extracellular and intracellular routes. [29, 56] Initially recognized by the formation of an orange red color (Fig. 2), the extracellular production of SeNPs by *Aspergillus terreus* H1 was confirmed as stated by Hussein *et al*. (2022) [57].

Zeta potential of the SeNPs formed, measured by PCS, showed a negative potential of (−25.6 mV) at pH 7. That suggests a stable colloidal was prepared. Zeta potential tracked the surface charges that SeNPs acquired; this allowed the colloidal SeNPs to remain stable. El-Saadony *et al*. (2021) reported that the magnitude of the zeta potential predicted prospective colloidal stability. The zeta potential of *L. paracasei*-SeNPs was determined to be 20.1 ± 0.6 Mv [58].

Data obtained from DLS showed that particles with an average size of 55.26±4 nm and a polydispersity index (PDI) of 0.465 were determined. That confirmed the formation of monodispersive SeNPs. Furthermore, the TEM micrograph results showed amorphous particles with a mean core size of 22.53±3 nm for SeNPs, which is consistent with the findings published by [58] [59, 60]**.**

The biological evaluation of SeNPs using *in vitro* cytotoxicity and anticancer activity assays have stated that the obtained SeNPs effectively has anticancer activity against the human lung adenocarcinoma cell line (A549) but are more safe, at the same time, on normal cells. These findings are in compliance with others obtained from previous studies using the sane cell line.[61, 62]**.**

For *in vivo* studies, the produced SeNPs were radiolabeled with the most common radioisotope used in radiopharmaceutical studies, ^{99m}Tc. SeNPs were readily and directly labeled, showing a radiochemical yield of 98.5 ± 0.5 in relatively normal conditions. The readiness of SeNPs to be radiolabeled with ^{99m}Tc may be attributed to their particle surfaces, which are capped with many fungal byproducts like polysaccharides, proteins, or peptides that contain functional groups such as -COOH, -OH, $-NH_2$, $-PO_3H_2$ and –SH and so react as chelating agents for ^{99m}Tc [63].

The nanoparticle shape, size and the capping materials are the main factors that affect pharmacokinetics, or biodistribution of nanomaterials [64]. Logically, smaller nanosizes facilitate longer blood circulation, as they can avoid reticuloendothelial system (RES) organs like liver and spleen, and enable passive targeting via the increased permeability and retention (EPR) effect in leaky tumor tissues [65]. When compared to normal cells, and regarding variations in hemostasis between normal body and a tumor bearing one, several cancer types exhibit higher concentrations of free radicals and ROS, so demanding elevated amounts of antioxidants and ROS-scavenging enzymes in order to prevent their apoptosis [66, 67], An adaptive reaction to intrinsic ROS stress may be the cause of this rise which could explain why antioxidant agents like selenium could be potential anticancer agents [68].

Conclusion

The current study has succeeded in easily isolating endophytic fungus *Aspergillus terreus* H1 from wild plant in Egypt *Rumex thyrsiflorus*, that used for obtaining biogenic SeNPs with excellent physical and biological characteristics, which could enable them to become an effective nanoplatform for molecular imaging of some tumor tissues, like lung cancer, by radiolabelling them with a 99-m-technetium radioisotope.

Acknowledgment(s)

The authors thank, Biotechnology lab, Botany and Micrbiology department, Al-azhar University (Girls branch) and Egyptian Atomic Energy Authority, Labeled Compounds Department members staff, for their contribution and technical support.

Author contributions

Heba I. Elkhouly: Writing-review & editing, Methodology, Investigation, Formal analysis, Data curation, Conceptulization, Ressources, Software, Validation, Visualization; **Zainab.S. Nasr:** Writing-review & editing, Methodology, Investigation, Formal analysis, Data curation, Conceptulization, Ressources, Software, Validation, Visualization; **Mohamed K. Hassane:** c Writing-review & editing, Methodology, Investigation, Formal analysis, Data curation, Conceptulization, Ressources, Software, Validation, Visualization.

Funding

The authors have not disclosed any funding.

Declaration

Authors declare that they have no conflict of interest as well as this study was performed in line with the principles of the declaration of Helsinki. Approval was granted by Research Ethics committee (REC) of Egyptian Atomic Energy Authority.

Abbreviations

rRNA: Ribosomal Ribonucleic Acid; DNA: Deoxyribonucleic Acid; BLAST: Basic Local Alignment Search Tool; NCBI: National Center for Biotechnology Information (MRC-5): normal human lung fibroblast cells; (A549): human lung adenocarcinoma cell line;

SeNPs: selenium nanoparticles; (Se): semi-metallic element selenium; (Na_2SeO_3) inorganic forms like selenite and selenite; (SeMet): selenomethionine; (SeCyt): selenocysteine; (GPx): glutathione peroxidase; (Na_2SeO_4): sodium selenite; (^{99m}Tc): technetium 99m; (RCY%): The percent radiochemical yield (REC/NCRRT): Research Ethics Committee.

References

[1] S.P. S, H.A. Rudayni, A. Bepari, S.K. Niazi, S. Nayaka, Green synthesis of Silver nanoparticles using Streptomyces hirsutus strain SNPGA-8 and their characterization, antimicrobial activity, and anticancer activity against human lung carcinoma cell line A549, Saudi journal of biological sciences, 29 (2022) 228-238.

[2] K.S. Siddiqi, A. Ur Rahman, Tajuddin, A. Husen, Properties of Zinc Oxide Nanoparticles and Their Activity Against Microbes, Nanoscale research letters, 13 (2018) 141.

[3] S.E. Sumner, R.L. Markley, G.S. Kirimanjeswara, Role of Selenoproteins in Bacterial Pathogenesis, 192 (2019) 69-82.

[4] J.J.O. Garza-García, J.A. Hernández-Díaz, A. Zamudio-Ojeda, J.M. León-Morales, A. Guerrero-Guzmán, D.R. Sánchez-Chiprés, J.C. López-Velázquez, S. García-Morales, The Role of Selenium Nanoparticles in Agriculture and Food Technology, 200 (2022) 2528-2548.

[5] H.G. Lazcano-Ramírez, J.J.O. Garza-García, J.A. Hernández-Díaz, Antifungal Activity of Selenium Nanoparticles Obtained by Plant-Mediated Synthesis, 12 (2023).

[6] L. Breydo, Selenium, Biologically Active Compounds, in: R.H. Kretsinger, V.N. Uversky, E.A. Permyakov (Eds.) Encyclopedia of Metalloproteins, Springer New York, New York, NY, 2013, pp. 1919-1924.

[7] T.M. Sakr, M. Korany, K.V. Katti, Selenium nanomaterials in biomedicine—An overview of new opportunities in nanomedicine of selenium, Journal of Drug Delivery Science and Technology, 46 (2018) 223-233.

[8] R. Abdulah, K. Miyazaki, M. Nakazawa, H. Koyama, Chemical forms of selenium for cancer prevention, Journal of Trace Elements in Medicine and Biology, 19 (2005) 141-150.

[9] L. Tan, X. Jia, X. Jiang, Y. Zhang, H. Tang, S. Yao, Q. Xie, In vitro study on the individual and synergistic cytotoxicity of adriamycin and selenium nanoparticles against Bel7402 cells with a quartz crystal microbalance, Biosensors & bioelectronics, 24 (2009) 2268-2272.

[10] R.S. Soumya, V.P. Vineetha, P.L. Reshma, K.G. Raghu, Preparation and Characterization of Selenium Incorporated Guar Gum Nanoparticle and Its Interaction with H9c2 Cells, PLOS ONE, 8 (2013) e74411.

[11] L. Sarin, V.C. Sanchez, A. Yan, A.B. Kane, R.H. Hurt, Selenium-carbon bifunctional nanoparticles for the treatment of malignant mesothelioma, Adv Mater, 22 (2010) 5207-5211.

[12] B. Hanson, G.F. Garifullina, S.D. Lindblom, A. Wangeline, A. Ackley, K. Kramer, A.P. Norton, C.B. Lawrence, E.A.H. Pilon-Smits, Selenium accumulation protects Brassica juncea from invertebrate herbivory and fungal infection, The New phytologist, 159 (2003) 461-469.

[13] M.F. Alam, M.M. Safhi, S.S. Moni, A. Jabeen, In Vitro Antibacterial Spectrum of Sodium Selenite against Selected Human Pathogenic Bacterial Strains, Scientifica, 2016 (2016) 9176273.

[14] S. Emrani, R. Zhiani, M. DafeJafari, The Biosynthesis of Silver Nanoparticles Using Plants of Glycyrrhiza glabra and Mentha Piperata and Its Antimicrobial Effect on Some Bacterias That Cause Tooth Decay, Journal of Rafsanjan University of Medical Sciences, 16 (2018) 953-968.

[15] B. Hosnedlova, M. Kepinska, S. Skalickova, C. Fernandez, B. Ruttkay-Nedecky, Q. Peng, M. Baron, M. Melcova, R. Opatrilova, J. Zidkova, G. Bjørklund, J. Sochor, R. Kizek, Nano-selenium and its nanomedicine applications: a critical review, International Journal of Nanomedicine, 13 (2018) 2107-2128.

[16] M.P. Rayman, Selenium and human health, Lancet (London, England), 379 (2012) 1256-1268.

[17] M. Korany, F. Marzook, B. Mahmoud, S.A. Ahmed, S.M. Ayoub, T.M. Sakr, Exhibiting the diagnostic face of selenium nanoparticles as a radio-platform for tumor imaging, Bioorganic Chemistry, 100 (2020) 103910.

[18] M. Korany, B. Mahmoud, S.M. Ayoub, T.M. Sakr, S.A. Ahmed, Synthesis and radiolabeling of vitamin C-stabilized selenium nanoparticles as a promising approach in diagnosis of solid tumors, Journal of Radioanalytical and Nuclear Chemistry, 325 (2020) 237-244.

[19] M.H. Bafghi, R. Nazari, M. Darroudi, e. al., Biosynthesis of selenium nanoparticles by Aspergillus flavus and Candida albicans and comparison of their effects with antifungal drugs, Research Square (2021).

[20] H. Abbas, D. Abou Baker, Biological Evaluation of Selenium Nanoparticles biosynthesized by Fusarium semitectum as antimicrobial and anticancer agents, Egyptian Journal of Chemistry, 63 (2019) 1119-1133.

[21] M. Kitching, M. Ramani, E. Marsili, Fungal biosynthesis of gold nanoparticles: mechanism and scale up, Microbial biotechnology, 8 (2015) 904-917.

[22] K. Bai, B. Hong, Z. Hong, J. Sun, C. Wang, Selenium nanoparticles-loaded chitosan/citrate complex and its protection against oxidative stress in d-galactose-induced aging mice, Journal of Nanobiotechnology, 15 (2017) 92.

[23] H.G. Wang, T. Dyakowski, P. Senior, R.S. Raghavan, W.Q. Yang, Modelling of batch fluidised bed drying of pharmaceutical granules, Chemical Engineering Science, 62 (2007) 1524-1535.

[24] A. R, V. Thazhenandayipurath, A. Jose, R. Krishnankutty, V. Vinod, Benefits of plant-endophyte interaction for sustainable agriculture, 2020, pp. 35-55.

[25] D.C. Wilson, Endophyte: The Evolution of a Term, and Clarification of Its Use and Definition, Oikos, 73 (1995) 274-276.

[26] E. Martinez-Klimova, K. Rodríguez-Peña, S. Sánchez, Endophytes as sources of antibiotics, Biochemical pharmacology, 134 (2017) 1-17.

[27] I.E. Heba, A.H. Ahmed, M.E.H. Asmaa, A.G. Mosad, M.S. Nagwa, Bioactive Secondary Metabolite from Endophytic Aspergillus Tubenginses ASH4 Isolated from Hyoscyamus muticus: Antimicrobial, Antibiofilm, Antioxidant and Anticancer Activity, Pharmacognosy Journal, 13 (2021).

[28] P.-K. Kyeremeh, K. Owusu, M. Ofosuhene, M. Ohashi, J. Agyapong, A. Sazak, M. Camas, Anti-Proliferative and Anti-Plasmodia Activity of Quinolactacin A2, Citrinadin A and Butrecitrinadin co-isolated from a Ghanaian Mangrove Endophytic Fungus Cladosporium oxysporum strain BRS2A-AR2F, Journal of Chemistry & Applications ,3 (2017).
[29] B. Zare, S. Babaie, N. Setayesh, A.R. Shahverdi, Isolation and characterization of a fungus for extracellular synthesis of small selenium nanoparticles, Nanomedicine Journal, 1 (2013) 13-19.
[30] M.M. Gharieb, A.M. Soliman, M.S. Omara, Biosynthesis of selenium nanoparticles by potential endophytic fungi Penicillium citrinum and Rhizopus arrhizus: characterization and maximization, Biomass Conversion and Biorefinery, (2023).
[31] S. Kumar, G. Stecher, K. Tamura, MEGA7: Molecular Evolutionary Genetics Analysis Version 7.0 for Bigger Datasets, Molecular Biology and Evolution, 33 (2016) 1870-1874.
[32] S. Yu, W. Zhang, W. Liu, W. Zhu, R. Guo, Y. Wang, D. Zhang, J. Wang, The inhibitory effect of selenium nanoparticles on protein glycation in vitro, Nanotechnology, 26 (2015) 145703.
[33] K.K. Vekariya, J. Kaur, K. Tikoo, ERα signaling imparts chemotherapeutic selectivity to selenium nanoparticles in breast cancer, Nanomedicine: Nanotechnology, Biology and Medicine, 8 (2012) 1125-1132.
[34] T. Mosmann, Rapid colorimetric assay for cellular growth and survival: application to proliferation and cytotoxicity assays, Journal of Immunological Methods, 65 (1983) 55-63.
[35] M.A. Motaleb, A.S.A. Adli, M. El-Tawoosy, M.H. Sanad, M. AbdAllah, An easy and effective method for synthesis and radiolabelling of risedronate as a model for bone imaging, Journal of Labelled Compounds and Radiopharmaceuticals, 59 (2016) 157-163.
[36] T.M. Sakr, M.E. Moustapha, M.A. Motaleb, 99mTc-nebivolol as a novel heart imaging radiopharmaceutical for myocardial infarction assessment, Journal of Radioanalytical and Nuclear Chemistry, 295 (2013) 1511-1516.
[37] H. Wongso, N. Zainuddin, I. Iswahyudi, Biodistribution and Imaging of The 99m Tc-Glutathione Radiopharmaceutical in White Rats Induced with Cancer, Atom Indonesia, 39 (2014) 106.
[38] K. Baba, J.L. Moretti, P. Weinmann, R. Senekowitsch-Schmidtke, M.T. Ercan, Tc-Glutathione Complex (Tc -GSH) : Labelling, Chemical Characterization and Biodistribution in Rats, Metal-Based Drugs, 6 (1999) 329-336.
[39] A. Vilchis-Juárez, G. Ferro-Flores, C. Santos-Cuevas, E. Morales-Avila, B. Ocampo-García, L. Díaz-Nieto, M. Luna-Gutiérrez, N. Jiménez-Mancilla, M. Pedraza-López, L. Gómez-Oliván, Molecular targeting radiotherapy with cyclo-RGDFK(C) peptides conjugated to 177Lu-labeled gold nanoparticles in tumor-bearing mice, J Biomed Nanotechnol, 10 (2014) 393-404.
[40] M.M. Swidan, T.M. Sakr, M.A. Motaleb, A. Abd El-Bary, M.T. El-Kolaly, Preliminary assessment of radioiodinated fenoterol and reproterol as potential scintigraphic agents for lung imaging, Journal of Radioanalytical and Nuclear Chemistry, 303 (2015) 531-539.
[41] M.M. Swidan, O.M. Khowessah, M.A. El-Motaleb, A.A. El-Bary, M.T. El-Kolaly, T.M. Sakr, Iron oxide nanoparticulate system as a cornerstone in the effective delivery of Tc-99 m radionuclide: a potential molecular imaging probe for tumor diagnosis, Daru : Journal of Faculty of Pharmacy, Tehran University of Medical Sciences, 27 (2019) 49-58.
[42] T.M. Sakr, O.M. Khowessah, M.A. Motaleb, A. Abd El-Bary, M.T. El-Kolaly, M.M. Swidan, I-131 doping of silver nanoparticles platform for tumor theranosis guided drug delivery, European journal of pharmaceutical sciences : Official Journal of the European Federation for Pharmaceutical Sciences, 122 (2018) 239-245.
[43] H.M. Rashed, I.T. Ibrahim, M.A. Motaleb, A.A. El-Bary, Preparation of radioiodinated ritodrine as a potential agent for lung imaging, Journal of Radioanalytical and Nuclear Chemistry, 300 (2014) 1227-1233.
[44] U.S. Yigit, F.Y. Lambrecht, P. Unak, F.Z. Biber, E.I. Medine, B. Cetinkaya, Preparation of (99m)Tc labeled vitamin C (ascorbic acid) and biodistribution in rats, Chemical & Pharmaceutical Bulletin, 54 (2006) 1-3.
[45] A. Vasas, O. Orbán-Gyapai, J. Hohmann, The Genus Rumex: Review of traditional uses, phytochemistry and pharmacology, Journal of Ethnopharmacology, 175 (2015) 198-228.
[46] K. Kalimuthu, R. Suresh Babu, D. Venkataraman, M. Bilal, S. Gurunathan, Biosynthesis of silver nanocrystals by Bacillus licheniformis, Colloids and Surfaces B: Biointerfaces, 65 (2008) 150-153.
[47] E. Piacenza, A. Presentato, E. Ambrosi, A. Speghini, R.J. Turner, G. Vallini, S. Lampis, Physical–Chemical Properties of Biogenic Selenium Nanostructures Produced by Stenotrophomonas maltophilia SeITE02 and Ochrobactrum sp. MPV1, Frontiers in Microbiology, 9 (2018).
[48] B.A. Khaw, H.W. Strauss, A. Carvalho, E. Locke, H.K. Gold, E. Haber, Technetium-99m labeling of antibodies to cardiac myosin Fab and to human fibrinogen, J Nucl Med, 23 (1982) 1011-1019.
[49] M. Santi, S.A.G. Lava, P. Camozzi, O. Giannini, G.P. Milani, G.D. Simonetti, E.F. Fossali, M.G. Bianchetti, P.B. Faré, The great fluid debate: saline or so-called "balanced" salt solutions?, Ital J Pediatr, 41 (2015) 47-47.
[50] C. Svensén, P. Rodhe, Chapter 33 - Intravascular Volume Replacement Therapy, in: H.C. Hemmings, T.D. Egan (Eds.) Pharmacology and Physiology for Anesthesia, W.B. Saunders, Philadelphia, 2013, pp. 574-592.
[51] J.P. Almeida, A.L. Chen, A. Foster, R. Drezek, In vivo biodistribution of nanoparticles, Nanomedicine (London, England), 6 (2011) 815-835.
[52] K. Loeschner, N. Hadrup, M. Hansen, S.A. Pereira, B. Gammelgaard, L.H. Møller, A. Mortensen, H.R. Lam, E.H. Larsen, Absorption, distribution, metabolism and excretion of selenium following oral administration of elemental selenium nanoparticles or selenite in rats, Metallomics, 6 (2014) 330-337.
[53] S.K. Nune, P. Gunda, P.K. Thallapally, Y.-Y. Lin, M.L. Forrest, C.J. Berkland, Nanoparticles for biomedical imaging, Expert Opin Drug Deliv, 6 (2009) 1175-1194.
[54] Q. Li, F. Liu, M. Li, C. Chen, G.M. Gadd, Nanoparticle and nanomineral production by fungi, Fungal Biology Reviews, 41 (2022) 31-44.
[55] Y.Y. Yuan, C.Q. Mao, X.J. Du, J.Z. Du, F. Wang, J. Wang, Surface charge switchable nanoparticles based on zwitterionic polymer for enhanced drug delivery to tumor, Adv Mater, 24 (2012) 5476-5480.

[56] J. Sarkar, P. Dey, S. Saha, K. Acharya, Mycosynthesis of selenium nanoparticles, Micro & Nano Letters, IET, 6 (2011) 599-602.
[57] H.G. Hussein, E.-S.R. El-Sayed, N.A. Younis, A.E.H.A. Hamdy, S.M. Easa, Harnessing endophytic fungi for biosynthesis of selenium nanoparticles and exploring their bioactivities, AMB Express, 12 (2022) 68.
[58] M.T. El-Saadony, A.M. Saad, T.F. Taha, A.A. Najjar, N.M. Zabermawi, M.M. Nader, S.F. AbuQamar, K.A. El-Tarabily, A. Salama, Selenium nanoparticles from Lactobacillus paracasei HM1 capable of antagonizing animal pathogenic fungi as a new source from human breast milk, Saudi Journal of Biological Sciences, 28 (2021) 6782-6794.
[59] H. Zhang, H. Zhou, J. Bai, Y. Li, J. Yang, Q. Ma, Y. Qu, Biosynthesis of selenium nanoparticles mediated by fungus Mariannaea sp. HJ and their characterization, Colloids and Surfaces A: Physicochemical and Engineering Aspects, 571 (2019) 9-16.
[60] N. Srivastava, M. Mukhopadhyay, Biosynthesis and structural characterization of selenium nanoparticles mediated by Zooglea ramigera, Powder Technology, 244 (2013) 26-29.
[61] K.A. Foster, C.G. Oster, M.M. Mayer, M.L. Avery, K.L. Audus, Characterization of the A549 Cell Line as a Type II Pulmonary Epithelial Cell Model for Drug Metabolism, Experimental Cell Research, 243 (1998) 359-366.
[62] J. Poofery, P. Khaw-On, Potential of Thai Herbal Extracts on Lung Cancer Treatment by Inducing Apoptosis and Synergizing Chemotherapy, Molecules, 25 (2020).
[63] G. Stöcklin, S.M. Qaim, F. Rösch, The Impact of Radioactivity on Medicine Metallic, Radiochimica Acta, 70-71 (1995) 249-272.
[64] K.O. Mohamed, Y.M. Nissan, A.A. El-Malah, W.A. Ahmed, D.M. Ibrahim, T.M. Sakr, M.A. Motaleb, Design, synthesis and biological evaluation of some novel sulfonamide derivatives as apoptosis inducers, European Journal of Medicinal Chemistry, 135 (2017) 424-433.
[65] J. Estrela, A. Ortega, E. Obrador, Estrela JM, Ortega A, Obrador EGlutathione in cancer biology and therapy. Crit Rev Clin Lab Sci 43: 143-181, Critical reviews in Clinical Laboratory Sciences, 43 (2006) 143-181.
[66] A. Thyagarajan, R.P. Sahu, Potential Contributions of Antioxidants to Cancer Therapy: Immunomodulation and Radiosensitization, Integr Cancer Ther, 17 (2018) 210-216.
[67] A. Sznarkowska, A. Kostecka, K. Meller, K.P. Bielawski, Inhibition of cancer antioxidant defense by natural compounds, Oncotarget, 8 (2017) 15996-16016.
[68] X. Wu, J. Cheng, X. Wang, Dietary Antioxidants: Potential Anticancer Agents, Nutrition and cancer, 69 (2017) 521-533.